# Tuning Catalytic Activity in the Hydrogenation of Unactivated Olefins with Transition-Metal Oxos as the Lewis Base Component of Frustrated Lewis Pairs

Nikola S. Lambic, Roger D. Sommer, and Elon A. Ison*

Department of Chemistry, North Carolina State University, 2620 Yarbrough Drive, Raleigh, North Carolina 27695-8204, United States

Ⓢ Supporting Information

ABSTRACT: The steric and electronic demands of the catalytic olefin hydrogenation of *tert*-butylethylene with oxorhenium/Lewis acid FLPs were evaluated. The sterics of the ligand were altered by installing bulkier isopropyl groups in the 2,6-positions of the diamidopyridine (DAP) ligand. Lewis acid/base adducts were not isolated for complexes with this ligand; however, species incorporating isopropyl groups were still active in catalytic hydrogenation. Modifications were also made to the Lewis acid, and catalytic reactions were performed with Piers' borane, $HB(C_6F_5)_2$, and the aluminum analogue $Al(C_6F_5)_3$. The rate of catalytic hydrogenation was shown to strongly correlate with the size of the alkyl, aryl, or hydride ligand. This was confirmed by a linear Taft plot with the steric sensitivity factor $\delta = -0.57$, which suggests that reaction rates are faster with sterically larger X substituents. These data were used to develop a catalyst $((MesDAP)Re(O)(Ph)/HB(C_6F_5)_2)$ that achieved a TON of 840 for the hydrogenation of *tert*-butylethylene at mild temperatures (100 °C) and pressures (50 psi of H_2). Tuning of the oxorhenium catalysts also resulted in the hydrogenation of *tert*-butylethylene at room temperature.
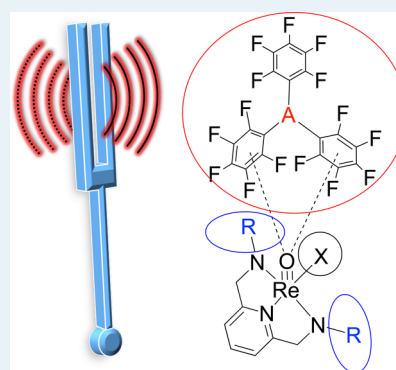
KEYWORDS: frustrated Lewis pairs, transition metal oxos, hydrogenation, olefins, catalytic tuning

INTRODUCTION

Since its discovery a decade ago, the chemistry of frustrated Lewis pairs (FLPs) has emerged as a powerful method for metal-free H_2 activation and has been utilized in a variety of catalytic reactions.[1] The most common catalytic reaction reported for FLPs is hydrogenation; as a result, many catalytic hydrogenations of unsaturated substrates, such as imines,[1d,h,i,l−n,p,q,2] silyl enol ethers,[1i,m,3] activated olefins,[1c,i,2b,4] and carbonyl-containing compounds[2d,5] have been described in the literature. However, the FLP-catalyzed hydrogenation of simple olefins remains a major challenge.[1c,2b,4g,j,o,6]

FLP olefin hydrogenation usually features combinations of boranes as the Lewis acid and main-group Lewis bases such as amines and phosphines. Catalytic hydrogenation with these FLPs is believed to proceed via initial heterolytic cleavage of H_2 to generate, in the case of phosphorus−boron FLPs, a hydridoborate/phosphonium salt. This species can protonate an olefin, to generate a stable cation that can accept a hydride from $HB(C_6F_5)_3$, resulting in the generation of the product (Scheme 1).[1c,2b,4g,j,o,6] Electron-rich olefins or olefins that are highly activated such as 1,1-diphenylethylene are typically employed to stabilize the carbocation intermediate that results from protonation. As a result, catalytic hydrogenation with main-group FLPs are generally not effective with unactivated olefins.

## Scheme 1. Proposed Mechanism for FLP (Phosphorus/Borane) Catalyzed Hydrogenation
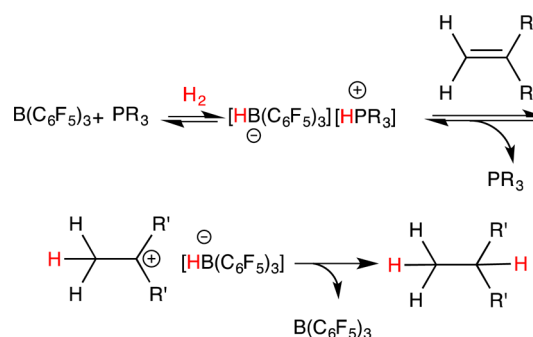
Our group recently reported an effective FLP where oxorhenium complexes were featured as the Lewis base component and $B(C_6F_5)_3$ was the Lewis acid and has shown that this system is capable of the hydrogenation of unactivated olefins such as ethylene, propylene, and 1-hexene.[7] The mechanism for this reaction was elucidated with experimental and computational data and proceeds by initial syn olefin addition to the FLP, followed by H_2 cleavage (Scheme 2). The

Scheme 2. Summary of the Proposed Mechanism for the Catalytic Hydrogenation of Olefins with FLPs Generated from Transition Metal Oxos

Scheme 3. Strategy for Examining the Sterics and Electronics in Oxorhenium FLPs
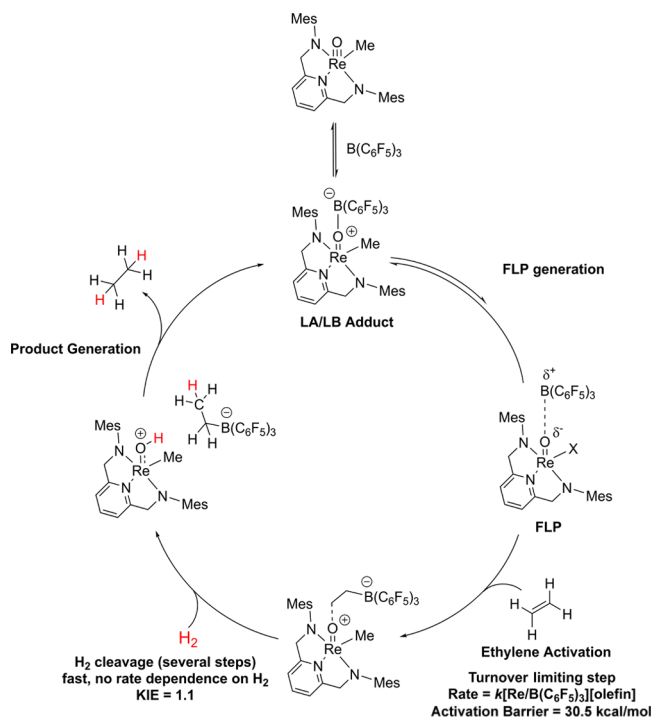

generation of an acidic rhenium hydroxyl as a result of H_2 splitting is the driving force for the final proton transfer that releases the hydrogenated product. Most notably, this new catalytic system was shown to be effective with low catalyst loadings (5 mol %) and low hydrogen pressures (50 psi). This is in contrast to the case for traditional FLPs, which typically operate at high catalyst loadings (20 mol %) and much higher H_2 pressures (50 bar). Thus, by utilizing a system that involves initial activation of the olefin followed by H_2 activation, it appears that we have addressed some of the challenges with traditional FLPs and the hydrogenation of unactivated olefins.

In this paper, we carried out additional experimental studies on this new FLP system. The modular nature of oxorhenium Lewis acid/base adducts allows for steric and electronic modifications on the diamidopyridine ligand, as well as the Lewis acid. These variations would ultimately lead to further improvements in the catalytic system and allow for an understanding of the factors that affect catalytic activity (Scheme 3).

The steric demands of the diamidopyridine ligand are examined first by synthesizing a series of complexes that incorporate the ligand DippDAP (DippDAP = 2,6-bis(2,6-bis((2,6-diisopropylphenyl)amino)methyl)pyridine)[8] and comparing their activities with those of the mesityl-substituted version of the ligand in the original complex.[7] Next, we examined the effect of altering both the steric and electronic demands of the borane component of the FLP by investigating reactions with $HB(C_6F_5)_2$, Piers' borane.[9] Finally, we examine the electronic effect of varying the central atom in the group III Lewis acids $B(C_6F_5)_3$ and $Al(C_6F_5)_3$.[10] The results obtained from these studies are critical for the rational design of new catalysts for this new type of FLP.
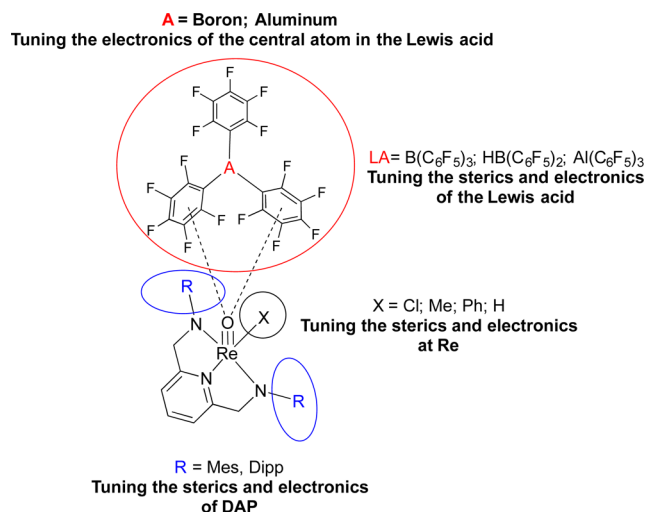
RESULTS AND DISCUSSION

Effect of Sterics of the Diamidopyridine Ligand. *Synthesis of (DippDAP)Re(O)X Complexes.* The DippDAP ligand (2,6-bis(2,6-bis((2,6-diisopropylphenyl)amino)methyl)-pyridine) was synthesized by an S_N2 substitution on the tosylated precursor with lithium (2,6-diisopropylphenyl)amide according to Scheme 4. The synthesized ligand was obtained in 62% yield, and the ^{1}H NMR data were consistent with the previously reported spectrum.[8b]
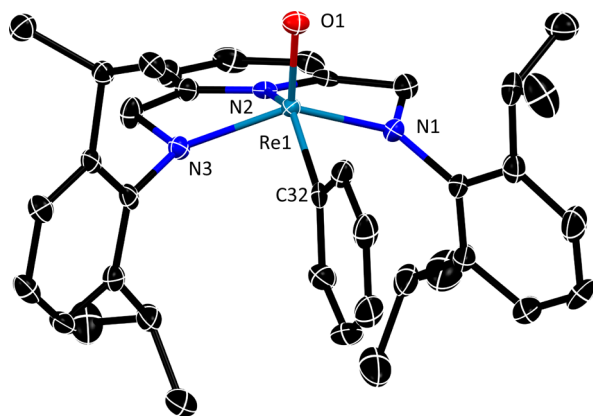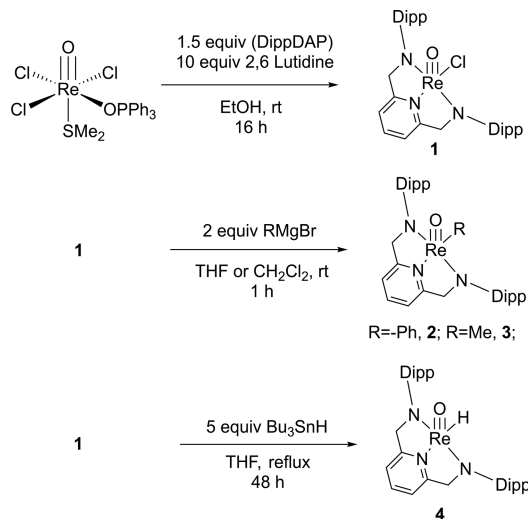
Scheme 4. Synthesis of DippDAP Ligand
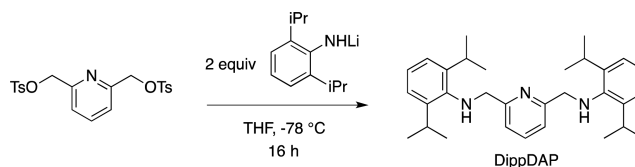
Rhenium complexes bearing the DippDAP ligand were synthesized utilizing the procedure previously reported for (MesDAP)Re(O)X type complexes (Scheme 5).[11] Complex **1** was successfully used as a precursor for new complexes incorporating a phenyl ligand (**2**) and a methyl ligand (**3**), as well as a hydride ligand (**4**), whose synthesis was reported elsewhere.[8a] X-ray-quality crystals of complex **2** were obtained by slow diffusion of pentane into a concentrated methylene chloride solution of the complex. The thermal ellipsoid plot of complex **2** is depicted in Figure 1. Bond lengths and angles are consistent with those in previously reported structures.[7,11,12]

The ligand environment around the rhenium center in complexes **1−4** can be easily confirmed by ^{1}H NMR spectroscopy, since the methylene protons become diastereotopic upon coordination of the ligand, leading to additional coupling and splitting of the protons oriented syn or anti to the rhenium oxo bond. Additionally, all complexes have two sets of isopropyl resonances by ^{1}H NMR spectroscopy, which further confirms the different chemical environments imposed on these protons, as a result of ligand coordination. The addition of Lewis acids such as $B(C_6F_5)_3$ to **1−4** resulted in the broadening of peaks in the ^{19}F NMR spectrum, reflecting the increased steric protection of the rhenium oxo moiety by much bulkier
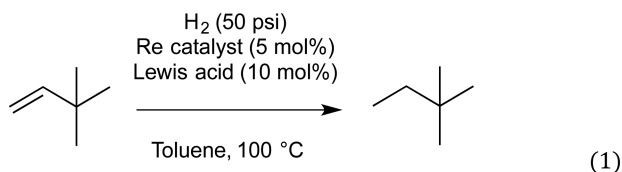
Scheme 5. Synthesis of Oxorhenium DippDAP Complexes

Figure 2. Conversions determined by ^1H NMR spectroscopy by integrating the ratio of *tert*-butyl singlets of the reactant and product. Conditions: Re-X (X = Ph (**1**), Me (**2**), Cl (**3**), H (**4**); 0.0046 mmol), and Lewis acid (0.0092 mmol), olefin (0.092 mmol) in a J. Young tube.

Figure 1. Thermal ellipsoid plot for **2** (50% probability ellipsoids). Selected bond lengths (Å): Re−N1, 1.978(2); Re−N2, 2.077(2); Re−N3, 1.983(2); Re−O1, 1.684(2); Re−C32, 2.082(3).
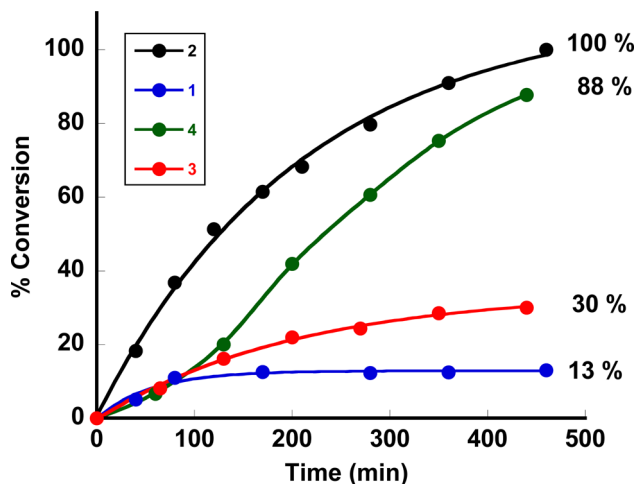
isopropyl substituents on the amide ligand. However, unlike the case for the analogous MesDAP complexes, adducts of Lewis acids could not be isolated with the DippDAP ligand.

Hydrogenation of tert-Butylethylene using Catalysts 1−4. In order to explore the effect of ligand sterics on the rates of hydrogenation of our model substrate *tert*-butylethylene, kinetic data were obtained and compared to those of the previously reported (MesDAP)Re(O)X complexes.[7] Complexes **1−4** were tested as catalysts under an H_2 atmosphere according to eq 1.

$$
\begin{array}{c}
H_2 \text{ (50 psi)} \\
\text{Re catalyst (5 mol\%)} \\
\text{Lewis acid (10 mol\%)} \\
\hline
\text{Toluene, 100 °C}
\end{array}
\qquad (1)
$$

Data for catalysts **1−4** are outlined in Figure 2 and, in general, are similar to the results reported for the MesDAP ligand. Catalyst **2** (Re−Ph) was again shown to be the most active catalyst (Figure 2). The observed rate constant, k_{obs}, was found to be 4.6×10^{-3} min^{-1}, which is slightly lower than the k_{obs} value (7.5×10^{-3} min^{-1}) for the MesDAP ligand.[7] Complexes bearing small, sterically unhindered X-type ligands such as methyl (**2**) and chloride (**1**) were poor catalysts in the
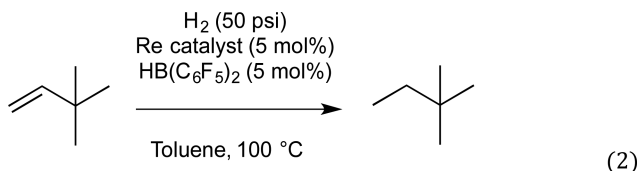
reaction, while the reaction catalyzed by a hydride complex (**4**) exhibited an induction period similar to that for the previously reported MesDAP complexes.[7] The activity of **4** can be similarly attributed to the additional reactions observed for MesDAPRe(O)(H), which resulted in the formation of more active catalysts such as Re alkyls, cyclometalated products, or pentafluorophenyl Re C_6F_5 derivatives.[7]

Significantly, it should be noted that adducts of $B(C_6F_5)_3$ could not be isolated with complexes incorporating the DippDAP ligand. Despite this observation, as shown in Figure 2, catalysis proceeded efficiently with these catalysts. This is consistent with notion that oxorhenium/$B(C_6F_5)_3$ Lewis acid base adducts do not lie on the catalytic cycle for hydrogenation.[13] Instead, a loosely bound frustrated Lewis pair is responsible for catalysis.

Altering the Steric and Electronic Demands of the Lewis Acid Component of the FLP. *Catalytic Hydrogenation with Piers' Borane.* In order to further investigate the effect of sterics and electronics on the catalytic hydrogenation of *tert*-butylethylene, the substituents at the boron center were altered. To do this, Piers' borane $HB(C_6F_5)_2$, a highly electrophilic reagent effective in hydroboration of olefins, was synthesized and utilized as the Lewis acid component of the FLP.[9] Replacement of one C_6F_5 group with a hydride substituent would allow for significant tuning of the electronics while still maintaining most of the necessary steric bulk required for the proposed FLP reactivity. Piers' borane was synthesized according to a modified literature procedure.[9]

Metal-free olefin hydrogenation was achieved by Wang and co-workers with Piers' borane as a catalyst.[4k] The substrate scope explored by this group is similar to that described in our previous study;[7] however, the conditions required to hydrogenate many substrates were harsh (6 bar of H_2, 120 °C, up to 72 h with 20 mol % of catalyst). The mechanism proposed involves hydroboration of the substrate, followed by H_2 cleavage via σ-bond metathesis. Given that $HB(C_6F_5)_2$ can serve as a catalyst, we carried out control studies with Piers' borane to determine whether or not olefins can be hydrogenated under the conditions described in eq 1 without the oxorhenium catalyst.

These control experiments revealed that olefin hydrogenation does not occur with Piers' borane under the optimized conditions employed here. However, when a variety of oxorhenium complexes were added, hydrogenation proceeded at overall improved rates for all complexes in comparison to the analogous reaction with $B(C_6F_5)_3$ as the Lewis acid component (eq 2).[7] The conditions were optimized to equimolar ratios of

$$\text{H}_2 \text{ (50 psi)}$$
$$\text{Re catalyst (5 mol\%)}$$
$$\text{HB(C}_6\text{F}_5)_2 \text{ (5 mol\%)}$$
$$\xrightarrow{\hspace{2cm}}$$
$$\text{Toluene, 100 °C}$$

(2)

rhenium and borane, respectively, yielding overall better conversions over time periods shorter than those for the corresponding reactions with $B(C_6F_5)_3$ (Figure 3).
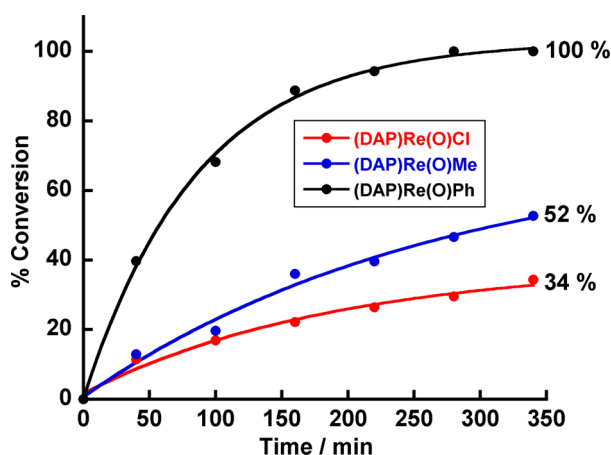
Figure 3. Conversions determined by ^{1}H NMR spectroscopy by integrating the ratio of *tert*-butyl singlets of the reactant and product. Conditions: Re-Ph (0.031 M), Lewis acid (0.061 M), and olefin (0.61 M) in a J. Young tube.

The conversion rates were found overall to be slightly faster in comparison to those in studies with $B(C_6F_5)_3$ as the Lewis acid component. For example, the k_{obs} value for the Re-Ph/$B(C_6F_5)_3$ pair was 7.5×10^{-3} min^{-1}, while k_{obs} for Re-Ph/$HB(C_6F_5)_2$ was 1.2×10^{-2} min^{-1}.

Mechanism with Piers' Borane. Since Piers' borane $HB(C_6F_5)_2$ contains a reactive B−H bond and has been shown to be active in olefin hydroboration, we examined whether the mechanism with complexes employing this Lewis acid was different.

Hydroboration of *tert*-butylethylene with Piers' borane occurs within minutes at room temperature. Therefore, the mechanism depicted in Scheme 6 begins with the hydroboration of *tert*-butylethylene to produce the new borane 3,3-dimethylbutyl-$B(C_6F_5)_2$. Addition of the FLP across the double bond in *tert*-butylethylene then occurs, followed by the subsequent addition of H$_2$, which eventually leads to the generation of product in a mechanism similar to that proposed earlier by us for oxorhenium/$B(C_6F_5)_3$ FLPs.[7]

Since the alkyl borane 3,3-dimethylbutyl-$B(C_6F_5)_2$ was easily generated from *tert*-butylethylene and Piers' borane, reactions with adducts of this Lewis acid and (MesDAP)Re(O)Ph were examined.

**Scheme 6. Proposed Mechanism for the Catalytic Hydrogenation with Piers' Borane as the Lewis Acid Component**
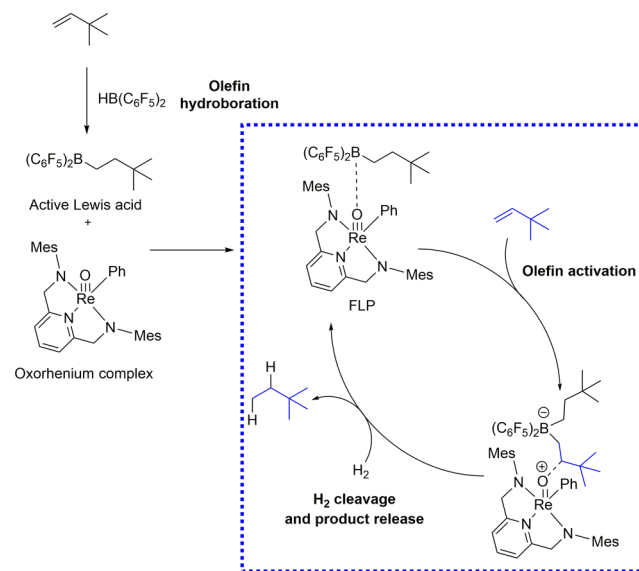
The kinetics of the catalytic hydrogenation of *tert*-butylethylene with the adduct $(C_6F_5)_2(3,3$-dimethylbutyl)B·(O)Re(MesDAP)(Ph) employed as a catalyst were examined by ^{1}H NMR spectroscopy (see the Supporting Information for details). The observed rate constant for this reaction, $k_{obs} = 2.1(4) \times 10^{-3}$ min^{-1}, was approximately 7 times slower than the rate constant obtained when Piers' borane was employed as the Lewis acid component, $1.5(2) \times 10^{-2}$ min^{-1}. While these results do not preclude the involvement of $(C_6F_5)_2(3,3$-dimethylbutyl)B·(O)Re(MesDAP)(Ph) as a catalyst, the data suggest that this species is not the primary component responsible for catalysis, as the catalytic rate with this species should be comparable to the rates obtained when Piers' borane was directly employed.

Synthesis of Oxorhenium Alane Lewis Acid/Base Adducts. In order to evaluate the electronic demands of the Lewis acid component and determine its effect on the rates of hydrogenation, we also synthesized traditional Lewis acid/base adducts of (MesDAP)Re(O)X with tris(pentafluorophenyl)-alane, $Al(C_6F_5)_3$ (Scheme 7).

Complexes **5**−**9** were isolated in modest to good yields (34−70%). All complexes exhibit the characteristic ^{1}H NMR resonances for the diastereotopic methylene backbone, which appear as two doublets. Other resonances are consistent with the previously reported ^{1}H NMR shifts for similar complexes.[7,8,12a] For example, the hydride ligand in complex **8** has a

Scheme 7. Synthesis of Lewis Acid/Base Adducts with $Al(C_6F_5)_3$

X = Ph, **5**; Me, **6**; Et, **7**; H, **8**; Cl, **9**
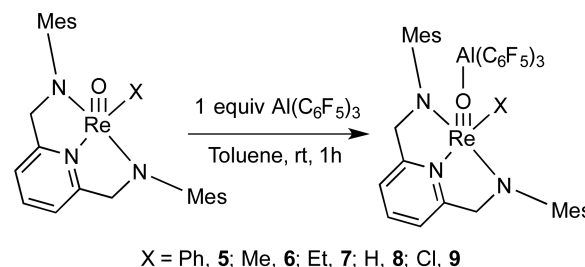
characteristic downfield shift in benzene-d_6 to 11.50 ppm, consistent with the coordination of the Lewis acid at the rhenium oxo.[8a] Interestingly enough, all complexes have identical ^{19}F NMR resonances at −123 ppm (t, 2F) −154 ppm (t, 1F), and −162 ppm (m, 2F), which are only slightly shifted from those of the parent $Al(C_6F_5)_3$.[8a] The synthesized complexes are not stable in the solid state, as traces of free oxorhenium complexes are observed in the matter of a few days.

X-ray Crystal Structure of 5. X-ray-quality crystals of **5** were obtained via the slow diffusion of pentane into a concentrated toluene solution at −40 °C. The thermal ellipsoid plot for **5** is shown in Figure 4. The structure and unit cell are similar to
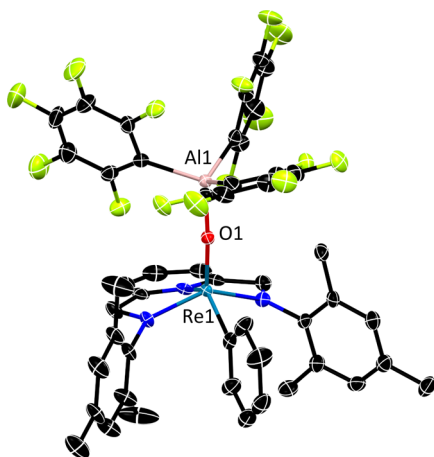

Figure 4. Thermal ellipsoid plot (50% probability ellipsoids) for complex **5**. Selected bond lengths (Å) and angles (deg): Re−O1, 1.765(4); Re−N1, 1.961(5); Re−N2, 2.025(5); Re−N3, 1.950(5); O1—Al1, 1.781(5); Al1−O1−Re1, 171.7(3).

those of the previously reported $(C_6F_5)_3B·(O)Re(MesDAP)-$(Ph).[7] The O−Al bond length in **5** is 1.780 Å. In contrast, the O−B bond length in $(C_6F_5)_3B·(O)Re(MesDAP)(Ph)$ is 1.534 Å. As a result, the structure of **5** is considerably more crowded than that of its boron analogue.[14]

Dynamic NMR Behavior of 5. The longer bond to aluminum is a result of its larger size (covalent radius) in comparison to that of boron. This is also evident in the ^{1}H NMR spectrum, as the difference in chemical shifts between the two diastereotopic protons of the MesDAP ligand is quite large (~0.83 ppm) in all Re=O/$B(C_6F_5)_3$ adducts, indicating the tight association of the Lewis acid to the oxorhenium Lewis base. This tight association results in substantially different chemical environments for the two diastereotopic protons. On the other hand, the difference in diastereotopic chemical shifts in the Re=O/$Al(C_6F_5)_3$ adducts is substantially smaller (0.69 ppm), which suggests that the aluminum Lewis acid is further away and therefore exhibits a lesser effect on the diastereotopic protons. This is also consistent with the observation in the solid state that the aluminum complexes are less sterically crowded than the analogous boron complexes (see Supporting Information).

When the ^{1}H NMR spectrum of **5** was examined from −80 to +100 °C, significant changes were observed (Figure 5). In the aromatic region, peaks were observed to sharpen and shift with increasing temperature. In addition, a peak at 5.4 ppm was observed to broaden and coalesce at approximately −15 °C ppm. This dynamic behavior is attributed to rotation of the
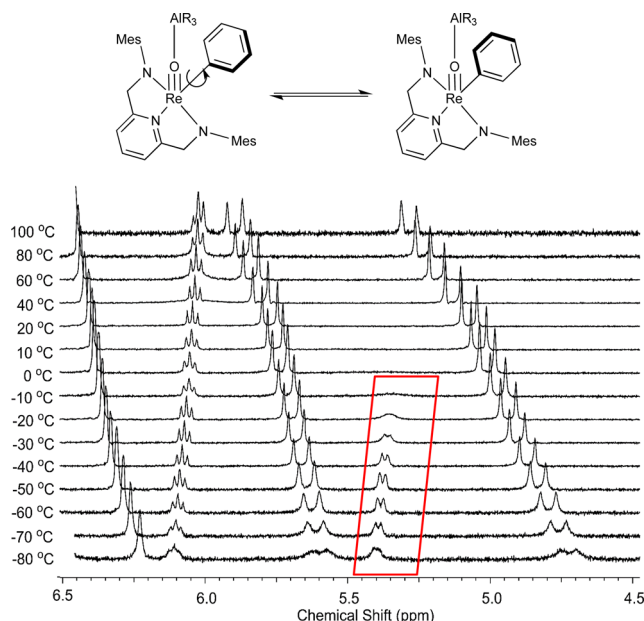
Figure 5. Variable-temperature spectrum of **5** from −80 to +100 °C.

phenyl ligand (Figure 5).[15] From the coalescence temperature and the chemical shift differences, a free energy of activation, $\Delta G^{\ddagger}$, of 13.5 kcal mol^{-1} was calculated. For the borane system this rotation was estimated to be 14.1 kcal mol^{-1}.[7] The smaller barrier to rotation calculated in the aluminum system is consistent with the observation from the crystal structure for **5** and provides further evidence that aluminum adducts are less sterically hindered.

Influence of Steric Parameters of the Re-X Fragment. The effect of the variation of the sterics of the X-type ligand bound to rhenium on the rates of hydrogenation of *tert*-butylethylene was investigated. Rate data were collected for complexes **5−9** according to eq 3, and the pseudo-first-order rate constants were extracted (Figure 6).

$$\text{(3)}$$
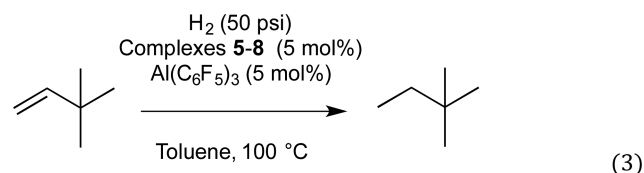
From Figure 6, it is evident that the sterics of the X-type ligand affect the rate of hydrogenation. For example, **5** was approximately 2−3 times faster as a catalyst than **6** and **7**, and about 15 times faster than the unsubstituted hydride catalyst **8**. Side reactions observed for the corresponding borane adducts (vide supra) were not observed for **8** and thus allowed for an examination of the steric effects of the hydride ligand. In addition, the overall rate of the reaction was approximately 3 times faster than the corresponding reaction with the boron system and roughly 2 times faster than the Re=O/Piers' borane system.

Taft's linear free energy relationship outlined in Taft's equation (eq 4) was utilized in order to examine the steric effects.[6]

$$\log\left(\frac{k}{k_{Me}}\right) = \rho^*\sigma^* + \delta E_s$$

$$\text{(4)}$$
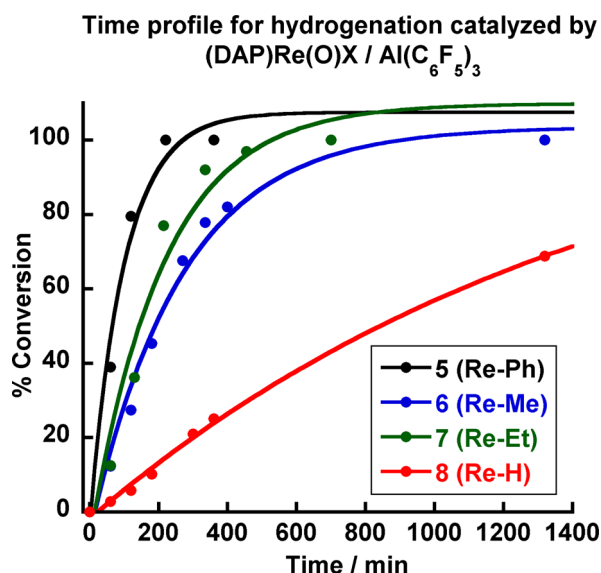
Figure 6. Conversions determined by ^{1}H NMR spectroscopy by integrating the ratio of *tert*-butyl singlets of the reactant and product. Conditions: Re complexes **5**−**8** (0.0046 mmol), Lewis acid (0.0046 mmol), and olefin (0.092 mmol) in a J. Young tube. $k_{obs}(\mathbf{5}) = [10(3)] \times 10^{-2}$ min^{-1}; $k_{obs}(\mathbf{6}) = [5(1)] \times 10^{-3}$ min^{-1}; $k_{obs}(\mathbf{7}) = [3.7(5)] \times 10^{-3}$ min^{-1}; $k_{obs}(\mathbf{8}) = [6.6(2)] \times 10^{-4}$ min^{-1}.

Assuming that the electronics of the oxorhenium species remain essentially unchanged by altering the alkyl, hydride, or aryl substituents in the Re-X position, the electronic factors $\rho^*\sigma^*$ will be negligible; thus, the equation simplifies to eq 5.

$$\log\left(\frac{k}{k_{Me}}\right) = \delta E_s \qquad (5)$$

Therefore, the plot of $\log(k/k_{Me})$ vs E_s will be linear with a slope of δ, the steric sensitivity factor. The pseudo-first-order rate constants were successfully correlated with Taft's steric parameter E_s[6] (Figure 7). The negative value of −0.57 obtained for δ suggests that the reaction is sensitive to the sterics of the X substituent. This is consistent with the hypothesis that the reaction rate is indeed accelerated by the increasing sterics in the Re-X position. High steric crowding in the proximity of the metal center prevents the tight association of the Lewis acid
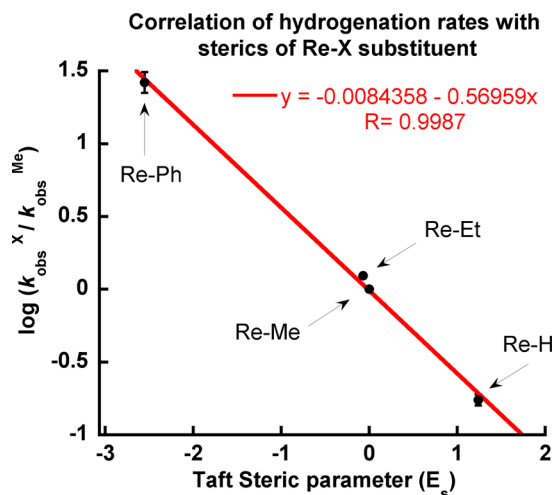
Figure 7. Taft plot of $\log(k_{obs}^X/k_{obs}^{Me})$ versus E_s.

with the Lewis basic Re=O and facilitates its dissociation to form a frustrated Lewis pair.

Thus, these data highlight critical design features in Re=O/Lewis acid FLPs. (1) Tight association of the Lewis acid/base should be avoided in order to allow facile access to an FLP, which is the catalytically active species. (2) Increased Lewis acidity appears to result in higher catalytic activity, as exemplified by the increased reaction rates with Al(C$_6$F$_5$)$_3$ and Piers' borane. (3) The nature of the central group 13 atom appears to be important. It appears that the larger covalent radius of aluminum in comparison to that of the boron analogues is critical. As noted above, aluminum analogues appear to be significantly less crowded sterically (see the Supporting Information). This is critical not only in allowing easy access to the catalytically active FLP but also in minimizing deactivation pathways that are available with the boron analogues.
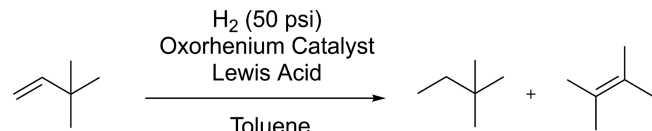
The Lewis acid Al(C$_6$F$_5$)$_3$ is more thermodynamically stable than B(C$_6$F$_5$)$_3$ and is less prone to previously observed deactivation pathways, such as protonation of the C$_6$F$_5$ fragment of the Lewis acid.[16] For example, little to no pentafluorobenzene (C$_6$F$_5$H) as a result of proton transfer from the acidic Re=OH moiety was observed in the aluminum system. The robustness of the Al-C$_6$F$_5$ fragments was noted in computational studies by Frenking and Timoshkin, where the formation of C$_6$F$_5$H as a result of intramolecular protonation was shown to be strongly exergonic for boron ($\Delta G° = -22.2$ kcal/mol) but only slightly exergonic for the corresponding aluminum Lewis acid ($\Delta G° = -1.4$ kcal/mol).[17] The elimination of these side reactions can account for the increased stability of the Re=O/Al(C$_6$F$_5$)$_3$ system.

The results outlined above can be used to rationally design new catalytic systems for olefin hydrogenation. As outlined in the next section, we utilize this strategy to develop unprecedented catalytic systems for olefin hydrogenations with an FLP.

3. Rational Design of Re=O/LA FLP for Olefin Hydrogenation. In contrast to polar substrates, the catalytic hydrogenation of unactivated olefins by FLPs remains a challenge. For example, Stephan and Paradies reported the hydrogenation of 1,1-diphenylethylene with a 20 mol % P/B FLP catalyst, where P = (C$_6$F$_5$)Ph$_2$P and B = B(C$_6$F$_5$)$_3$.[4o] The use of *p*TolNMe$_2$ as a base allowed the catalyst loading to be reduced to 5 mol %. The Paradies group extended FLP reductions to β-nitrostyrenes and acrylates using (2,6-C$_6$H$_3$F$_2$)$_3$B/2,6-lutidine (20 mol %) at 40 °C with H$_2$ (4 bar).[4g] Earlier this year we expanded the scope of unactivated olefins that can be hydrogenated with a Re=O/B FLP system using 5 mol % of catalyst at 100 °C.[7]

In this paper, we have shown that the modular nature of Re=O/B FLPs allows for easily tuned catalytic activity. Specifically, the sterics of the ligand were altered by installing bulkier isopropyl groups in the 2,6-positions of the diamido pyridine ligand. In addition, the sterics and electronics of the Lewis acid were altered by utilizing Piers' borane, HB(C$_6$F$_5$)$_2$. Finally, the nature of the central group 13 Lewis acid in M(C$_6$F$_5$)$_3$ (M = boron, aluminum) was investigated by synthesizing adducts with Al(C$_6$F$_5$)$_3$.

With these modifications we examined the catalytic hydrogenation of *tert*-butylethylene as depicted in Table 1. For these reactions we employed (O)Re(MesDAP)(Ph) and (O)Re-(DippDAP)(Ph) as the Lewis base components. In addition, B(C$_6$F$_5$), HB(C$_6$F$_5$)$_2$ and Al(C$_6$F$_5$)$_3$ were employed as the

Table 1. Catalytic Hydrogenation of *tert*-Butyl Ethylene with Re═O/Lewis Acid Frustrated Lewis Pairs[a]

entry	oxorhenium complex	Lewis acid	temp (°C)	loading (mol %)	conversion (%)[b]	TON	TOF (h^{-1})
1	(O)Re(MesDAP)Ph	B(C$_6$F$_5$)$_3$	100	0.6	100	169	4.0
2[c]	(O)Re(MesDAP)Ph	B(C$_6$F$_5$)$_3$	100	0.1	6	45	1.2
3	(O)Re(MesDAP)Ph	Al(C$_6$F$_5$)$_3$	100	0.6	100	169	4.0
4[c]	(O)Re(MesDAP)Ph	Al(C$_6$F$_5$)$_3$	100	0.1	16	130	3.4
5	(O)Re(MesDAP)Ph	HB(C$_6$F$_5$)$_2$	100	0.6	100	169	4.0
6[c]	(O)Re(MesDAP)Ph	HB(C$_6$F$_5$)$_2$	100	0.1	100	840	20
7	(O)Re(MesDAP)Ph	HB(C$_6$F$_5$)$_2$	80	0.6	100	169	4.0
8	(O)Re(MesDAP)Ph	HB(C$_6$F$_5$)$_2$	60	0.6	96	163	3.9
9	(O)Re(MesDAP)Ph	HB(C$_6$F$_5$)$_2$	20	0.6	20	25	0.6
10	(O)Re(DippDAP)Ph	B(C$_6$F$_5$)$_3$	100	0.6	93	156	3.7
11	(O)Re(DippDAP)Ph	Al(C$_6$F$_5$)$_3$	100	0.6	48	81	1.9
12	(O)Re(DippDAP)Ph	HB(C$_6$F$_5$)$_2$	100	0.6	87	146	3.5

[a]Conditions unless specified otherwise: oxorhenium (0.0046 mmol), Lewis acid (0.0092 mmol), and substrate (0.776 mmol) in toluene (0.5 mL) in a 25 mL Teflon sealed reaction vessel, pressurized with 50 psi of H$_2$. Conversions were determined by ^{1}H NMR spectroscopy. TON values are based on combined hydrogenation and isomerization catalysis. [b]2,3-Dimethylbut-2-ene (3−5%) was observed as a side product in all catalytic reactions. [c]3.83 mmol of substrate used.

Lewis acid components. Reactions were performed under H$_2$ (50 psi), and product formation was analyzed by ^{1}H NMR spectroscopy.

In the previous sections, we examined the effect of varying the sterics and electronics of the oxorhenium complex, as well as the Lewis acid component on the rate of the catalytic hydrogenation of *tert*-butylethylene. In Table 1, it is evident that these modifications also have an effect on catalyst stability. Consequently, a TON value of 840 was achieved with the (O)Re(MesDAP)(Ph)/HB(C$_6$F$_5$)$_2$ catalyst system (entry 6). In contrast, TON values of 45 and 130 were achieved with (O)Re(MesDAP)(Ph)/B(C$_6$F$_5$)$_3$ and the (O)Re(MesDAP)-(Ph)/Al(C$_6$F$_5$)$_3$, respectively. Thus, the trend in TONs is HB(C$_6$F$_5$)$_2$ > Al(C$_6$F$_5$)$_3$ > B(C$_6$F$_5$)$_3$. This trend appears to reflect the increased Lewis acidity of HB(C$_6$F$_5$)$_2$ and Al(C$_6$F$_5$)$_3$ and the stability of these Lewis acids with regard to protolytic cleavage of the C$_6$F$_5$ group to produce pentafluorobenzene.[17]

To the best of our knowledge, the type of activity reported in Table 1 is unprecedented for any reported catalytic FLP hydrogenation with an unactivated olefin. Furthermore, the TONs with Piers' borane are at least 5−6 times those of any reported FLP system thus far.

Modification of the Lewis acid also allows catalysis to be performed at lower temperatures (entries 7−9) with turnovers achievable at room temperature (entry 9). As noted earlier, catalysis was also possible with the DippDAP ligand (entries 10−12), even though Lewis acid/adducts with this ligand were not isolated. This lends further support to the notion that Lewis acid/base adducts do not lie on the catalytic cycle.

In all catalytic reactions 2−5% of 2,3-dimethylbut-2-ene was also observed. The presence of this substrate can be explained by isomerization of the *tert*-butylethylene in the presence of the Lewis acid via a methyl shift mechanism. To account for these observations, a modified mechanism has been proposed in Scheme 8. This mechanism begins with the activation of the olefin by the Lewis acid. This is similar to a report by Ménard and Stephan, where the first Al-olefin complex was isolated and shown to react with hydrides to form alkyls.[18]

Scheme 8. Proposed Mechanism for Re═O/Lewis Acid Catalyzed Olefin Hydrogenation
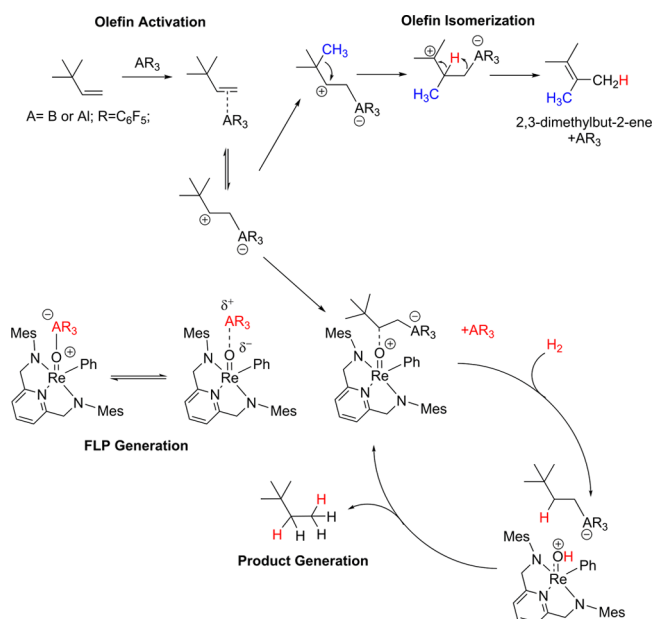
In this paper, it was noted: "if redistribution could be inhibited, the protic cation derived from FLP activation of H$_2$ could react with the transient alkylaluminate to provide an entry to a catalytic cycle for hydrogenation."[18b] In the current proposed mechanism the acidic species [(DAP)(Ph)Re═OH]$^+$ is generated that can protonate the anion [(alkyl)AR$_3$]$^-$ and generate the product. The barrier for this process was shown, via computational studies, to be reasonable.[7]

■ CONCLUSIONS

In conclusion, we have evaluated the steric and electronic demands of catalytic olefin hydrogenation with oxorhenium/Lewis acid FLPs. The sterics of the ligand were altered by installing bulkier isopropyl groups in the 2,6-positions of the

diamidopyridine (DAP) ligand. Increased crowding in the DAP ligand hinders the formation of Lewis acid/base adducts. However, species incorporating isopropyl groups were still active in the catalytic hydrogenation of *tert*-butylethylene. This is consistent with the hypothesis that Lewis acid/base adducts of oxorhenium complexes are not on the catalytic cycle and that the catalytically active species is a frustrated Lewis pair where noncovalent interactions between the Lewis base (oxorhenium complexes) and the Lewis acid account for the stability.

The reaction rates were slightly improved with Piers' borane, $HB(C_6F_5)_2$, and the aluminum analogue $Al(C_6F_5)_3$ with an overall 3-fold increase in the rate with aluminum attributed to factors such as (1) the increased Lewis acidity of aluminum, (2) the ease of Lewis acid dissociation, and (3) the minimization of decomposition pathways in the case of $Al(C_6F_5)_3$.

The rate of catalytic hydrogenation was shown to strongly correlate with the size of the alkyl, aryl, or hydride ligand. This was confirmed by a linear Taft plot with the steric sensitivity factor $\delta = -0.57$, which suggests that reaction rates are faster with a larger X-type ligand. Thus, high steric crowding in the proximity of the metal center prevents the tight association of the Lewis acid with the Lewis basic Re=O and facilitates its dissociation to form a frustrated Lewis pair.

These data were used to develop a catalyst ((MesDAP)Re-(O)(Ph)/HB(C_6F_5)_2) that achieved a TON value of 840 for the hydrogenation of *tert*-butylethylene at mild temperatures (100 °C) and pressures (50 psi of H_2). Tuning the oxorhenium catalysts also resulted in the hydrogenation of *tert*-butylethylene at room temperature. These results, to the best of our knowledge, are unprecedented for the catalytic hydrogenation of an unactivated olefin by an FLP. This lends further support to the notion that the modular nature of the oxorhenium complexes allows for efficient tuning of catalytic activity.[19]

■ EXPERIMENTAL SECTION

General Considerations. Ligands and oxorhenium chloride, phenyl, hydride, and methyl precursors were prepared as previously reported.[7,11,12b] $Al(C_6F_5)_3$[10] and $HB(C_6F_5)_2$[9] were synthesized according to modified literature procedures. $B(C_6F_5)_3$ was purchased from Strem Inc. and sublimed before use. All manipulations were performed using standard Schlenk and glovebox techniques. ^1H NMR spectra were recorded on a Varian Mercury 300 MHz spectrometer at room temperature. ^{13}C and ^{19}F NMR spectra were recorded on a Varian Mercury 400 MHz spectrometer at room temperature. X-ray data were collected by Dr. Roger Sommer (NCSU). FTIR spectra were recorded on a JASCO FT/IR-4100 instrument. Elemental analyses were performed by Atlantic Micro Laboratories, Inc.

General Procedure for Kinetic Analysis. In an oven-dried J. Young tube the rhenium complexes (0.0046 mmol) and the corresponding Lewis acids (0.0092 mmol, 2 equiv with respect to rhenium) were dissolved in 0.2 mL of deuterated toluene. 3,3-Dimethyl-1-butene (0.092 mmol) was then added to the J. Young tube via microsyringe, and the tube was degassed via three freeze−pump−thaw cycles. The J. Young tube was then pressurized with H_2 (50 psi, 99.996 purity grade) and placed in an oil bath. Conversions were determined by ^1H NMR spectroscopy by integrating the ratios of the *tert*-butyl singlet of the product with respect to the reactant.

General Procedure for Catalytic Reactions Described in Table 1. In an oven-dried 25 mL storage tube, the rhenium complex (0.0046 mmol) and the Lewis acid (0.0092 mmol, 2 equiv with respect to rhenium) were dissolved in 0.5 mL of

deuterated toluene. *tert*-Butylethylene (0.776 mmol, 100 μL or 3.88 mmol, 500 μL) was then added to the resulting solution, and the storage tube was degassed via three freeze−pump−thaw cycles. The tube was pressurized with H_2 (50 psi, 99.996 purity grade), and the resulting solutions were placed in a corresponding oil bath and stirred for 42 h. After it was cooled, the tube was depressurized and the reaction mixture was analyzed by ^1H NMR spectroscopy. Conversions were determined by integrating the ratios of the *tert*-butyl singlet of the product with respect to the reactant.

Synthesis of Pyridine-2,6-diylbis(methylene) Bis(4-methylbenzenesulfonate). In a 50 mL round-bottom flask, pyridine-2,6-dimethanol (700 mg, 5.04 mmol) was dissolved in 10 mL of a 1/1 mixture of THF and water and was cooled to 0 °C using an ice bath. NaOH (440 mg, 11.1 mmol) was then slowly added to the stirred reaction mixture, which was followed by the dropwise addition of a solution of TsCl in THF (1.92 g, 10.1 mmol, 8 mL of solution). The resulting cloudy mixture was stirred for 6 h at 0 °C. After 6 h, the reaction was warmed to room temperature and the product was extracted with 15 mL of CH_2Cl_2. The organic layer was then dried over anhydrous Na_2SO_4 and concentrated to give a white solid. Isolated yield: 1.95 g (86%). ^1H NMR ($CDCl_3$): δ 7.80 (d, *J* = 8.0 Hz, 4H, tosyl aromatic); 7.80 (d, *J* = 8.0 Hz, 4H, tosyl aromatic); 7.68 (t, *J* = 7.7 Hz, 1H, pyridine *para*-H); 7.32 (d, *J* = 8.0 Hz, 6H, tosyl aromatic/pyridine *meta*-H); 5.04 (s, 4H, Pyr CH_2); 2.44 (s, 6H, tosyl *para*-CH_3).

Synthesis of Pyridine-2,6-bis(diisopropylamine) (DippDAP). Following standard air-free techniques, in a 100 mL Schlenk flask, 2,6-diisopropylaniline (9.08 mmol, 1.7 mL) was dissolved in 20 mL of dry THF. To the cooled reaction mixture at −78 °C was added *n*-BuLi (9.08 mmol, 3.6 mL) dropwise, and the reaction mixture was warmed to room temperature. The reaction mixture was then cooled to −78 °C. The solution of tosylated pyridine (4.54 mmol, 2.03 g) in dry THF was then cannula-transferred to a solution of deprotonated aniline; this was instantly accompanied by a color change from yellow to dark orange. The resulting solution was stirred for 16 h. A saturated solution of NH_4Cl (30 mL) was then placed in the flask, and the product was extracted with ether (2 × 30 mL). The combined organic extracts were dried over Na_2SO_4 and then concentrated under vacuum to afford a yellow oil (1.28 g, 61% yield). ^1H NMR ($CDCl_3$): δ 7.68 (t, *J* = 7.9 Hz, 1H, Pyr *para*-H); 7.30 (d, *J* = 7.9 Hz, 2H, Pyr *meta*-H); 7.18 (m, *J* = 7.7 Hz, 1H, pyridine *para*-H); 7.32 (d, *J* = 8.0 Hz, 6H, tosyl aromatic/pyridine *meta*-H); 5.04 (s, 4H, Pyr CH_2−); 2.44 (s, 6H, tosyl *para*-CH_3).

Synthesis of (DippDAP)Re(O)Cl. In a 250 mL round-bottom flask, $(SMe_2)(OPPh_3)Re(O)Cl_3$ (450 mg, 0.693 mmol) and the DippDAP ligand (1.5 equiv, 1.04 mmol) were dissolved in 100 mL of absolute EtOH. 2,6-Lutidine (6.93 mmol, 0.8 mL) was added to the reaction mixture, which was stirred overnight at room temperature. Filtration afforded 151.6 mg (32% yield) of a green powder. Vapor diffusion of pentane into a concentrated solution of methylene chloride resulted in crystals suitable for X-ray analysis. ^1H NMR (CD_2Cl_2): δ 8.23 (t, *J* = 7.9 Hz, 1H, NC_2H_2CH); 7.87 (d, *J* = 7.7 Hz, 2H, NC_2H_2CH); 7.21−7.14 (m, 6H, aromatic); 5.60 (s, 4H, MesNCH_2); 3.88 (spt, *J* = 6.8 Hz, 2H, ^{i}Pr methine); 2.28 (spt, *J* = 6.8 Hz, 2H, ^{i}Pr methine); 1.30 (d, *J* = 6.9 *Hz*, 6H, iPr *CH_3*); 1.23 (d, *J* = 6.9 *Hz*, 6H, iPr *CH_3*); 1.02 (d, *J* = 6.9 Hz, 6H, iPr *CH_3*); 0.92 (d, *J* =6.9 Hz, 6H, iPr *CH_3*). ^{13}C NMR (CD_2Cl_2): δ 168.16, 153.94, 147.30, 146.31, 143.73, 126.26, 124.02, 123.61, 117.30, 82.40,

27.96, 27.38, 25.42, 25.03, 24.30. Anal. Calcd for $C_{31}H_{41}ClN_3ORe$: C, 53.70; N, 6.06, H, 5.9., Found: C, 53.83, N, 6.07, H, 6.13.

Synthesis of (DippDAP)Re(O)Ph. In a 25 mL scintillation vial (DippDAP)Re(O)Cl (91.0 mg, 0.131 mmol) was dissolved in 5 mL of CH_2Cl_2. In a glovebox, PhMgBr (2 equiv, 0.09 mL, 0.263 mmol) was added dropwise to the reaction mixture, which resulted in an immediate color change from green to brown. The reaction mixture was stirred under an inert atmosphere for 1 h, after which it was taken outside of the glovebox and quenched with 15 mL of DI water. The organic layer was separated, dried over Na_2SO_4, and concentrated to approximately 1 mL. Addition of excess pentane resulted in a brown precipitate, which was collected on a filter frit and dried under vacuum. Isolated yield: 53.1 mg (55%). Vapor diffusion of pentane into a concentrated CH_2Cl_2 solution resulted in X-ray-quality crystals. ^{1}H NMR (CD_2Cl_2): δ 8.18 (t, J = 7.9 Hz, 1H, NC_2H_2CH); 7.76 (d, J = 7.7 Hz, 2H, NC_2H_2CH); 6.92−6.88 (m, 6H, aromatic); 6.43 (t, J = 8.3 Hz, 2H, Ph-*ortho*); 6.02 (t, J = 7.3 Hz, 1H, Ph-*para*); 5.87 (d, J = 20.2 Hz, 2H, −NCH_2-Pyr) 5.77 (d, J = 20.2 Hz, 2H, −NCH_2-Pyr); 4.09 (spt, J = 6.8 Hz, 2H, ^{i}Pr methine); 2.26 (spt, J = 6.8 Hz, 2H, ^{i}Pr methine); 1.20 (d, J = 6.9 Hz, 6H, ^{i}Pr CH_3); 1.13 (d, J = 6.9 Hz, 6H, ^{i}Pr CH_3); 1.08 (d, J = 6.9 Hz, 6H, ^{i}Pr CH_3); 1.05 (d, J = 6.9 Hz, 6H, ^{i}Pr CH_3). ^{13}C NMR (CD_2Cl_2): δ 167.27, 153.67, 147.02, 145.37, 142.03, 133.04, 125.43, 125.27, 123.46, 123.02, 121.53, 116.66, 81.25, 27.77, 27.00, 26.93, 26.73, 24.26, 22.71, 22.57. Anal. Calcd for $C_{37}H_{46}N_3ORe·H_2O$: C, 59.02; H, 6.43; N, 5.58. Found: C, 59.11; H, 6.41; N, 5.39.

Synthesis of (DippDAP)Re(O)H. In a 25 mL pressure vessel (DippDAP)Re(O)Cl (100 mg, 0.14 mmol) was dissolved in 5 mL of dry THF in the glovebox. Tributyltin hydride (0.72 mmol, 0.2 mL) was added, and the reaction mixture was stirred at 80 °C for 2 days. When the mixture was cooled, solvent was removed under vacuum and the remaining residue was taken up in excess hexanes to precipitate the product as a red powder, which was filtered and dried under vacuum. Isolated yield: 70.5 mg (76%). ^{1}H NMR (CD_2Cl_2): δ 8.15 (t, J = 7.9 Hz, 1H, NC_2H_2CH); 7.70 (d, J = 7.7 Hz, 2H, NC_2H_2CH); 7.29 (s, 1H, Re-H); 7.14−7.09 (m, 6H, aromatic); 5.63 (d, J = 20.2 Hz, 2H, −NCH_2 Pyr); 5.52 (d, J = 20.2 Hz, 2H, −NCH_2 Pyr); 3.86 (spt, J = 5.8 Hz, 2H, iPr methine); 2.56 (spt, J = 5.8 Hz, 2H, iPr methine); 1.31 (d, J = 7.7 Hz, 6H, ^{i}Pr CH_3); 1.18 (d, J = 7.7 Hz, 6H, ^{i}Pr CH_3); 1.01 (d, J = 7.7 Hz, 6H, ^{i}Pr CH_3); 1.00 (d, J = 7.7 Hz 6H, ^{i}Pr CH_3). ^{13}C NMR (CD_2Cl_2): δ 169.0, 159.17, 147.10, 144.52, 141.49, 125.50, 124.04, 123.70, 116.66, 80.87, 27.54, 27.27, 25.36, 25.29, 24.33, 24.12. FTIR (KBr pellet): ν(Re-H) 2034 cm^{-1}. Anal. Calcd for $C_{31}H_{42}N_3ORe$: C, 56.51; H, 6.43; N, 6.38. Found: C, 55.97; H, 6.49; N, 6.26.

Synthesis of (DippDAP)Re(O)Me. In a 25 mL scintillation vial (DippDAP)Re(O)Cl (60.0 mg, 0.087 mmol) was dissolved in 5 mL of THF under an inert atmosphere. MeMgBr (2 equiv, 0.06 mL, 0.173 mmol) was added dropwise to the reaction mixture, which resulted in an immediate color change from green to purple. The reaction mixture was stirred under an inert atmosphere for 1 h, after which it was taken outside of the glovebox and quenched with 15 mL of DI water. The compound was extracted with 2 × 10 mL of CH_2Cl_2, and the organic layer was separated and dried over Na_2SO_4. Solvent was removed in vacuo, and addition of excess pentane resulted in a purple precipitate, which was collected on a filter frit and dried under vacuum. ^{1}H NMR (CD_2Cl_2): δ 8.08 (t, J = 7.9 Hz, 1H,

NC_2H_2CH); 7.72 (d, J = 7.7 Hz, 2H, NC_2H_2CH); 7.20−7.11 (m, 6H, aromatic); 5.64 (d, J = 20.2 Hz, 2H, −NCH_2 Pyr); 5.55 (d, J = 20.2 Hz, 2H, −NCH_2 Pyr); 3.90 (septet, J = 5.8 Hz, 2H, iPr methine); 2.18 (septet, J = 5.8 Hz, 2H, iPr methine); 2.13 (s, 3H, Re-Me); 1.31 (d, J = 7.7 Hz, 6H, ^{i}Pr CH_3); 1.18 (d, J = 7.7 Hz, 6H, ^{i}Pr CH_3); 1.01 (d, J = 7.7 Hz, 6H, ^{i}Pr CH_3); 1.00 (d, J = 7.7 Hz, 6H, ^{i}Pr CH_3). ^{13}C NMR (CD_2Cl_2): δ 168.50, 153.06, 147.90, 146.10, 141.30, 125.66, 124.17, 124.12, 123.40, 116.40, 81.74, 27.47, 27.03, 25.81, 25.60, 25.14, 23.71, 16.48.

Synthesis of (DAP)Re(Ph)(O)Al$(C_6F_5)_3$. A 100 mL Schlenk flask was charged with (DAP)Re(O)Ph (100 mg, 0.154 mmol) and Al$(C_6F_5)_3$·(toluene) (95.5 mg, 0.154 mmol, 1 equiv) and dissolved in 15 mL of toluene under an inert atmosphere. The resulting brown solution was stirred at room temperature for 1 h. The solvent volume was then reduced to ∼5 mL in vacuo, and excess hexanes (30 mL) was cannula-transferred into the flask, which precipitated a brown powder. The resulting mixture was stirred for another 30 min. Excess solvent was then cannula-filtered, leaving the brown powder in the flask, which was further dried in vacuo for 3 h. Isolated yield: 105 mg (0.089 mmol, 58%). ^{1}H NMR (C_6D_6): δ 6.91 (t, J = 8.0 Hz, 1H, NC_2H_2CH); 6.62 (t, J = 8.0 Hz, 2H, Ph *meta*-H); 6.54 (s, 2H, Mes *meta*-H); 6.53 (d, J = 8.0 Hz, 2H, NC_2H_2CH); 6.34 (s, 2H, Mes *meta*-H); 6.07 (t, J = 7.0 Hz, 1H, Ph *para*-H); 5.62 (d, J = 21.0 Hz, 2H, MesNCH_2); 4.96 (d, J = 21.0 Hz, 2H, MesNCH_2); 2.21 (s, 6H, Mes CH_3); 1.92 (s, 6H, Mes CH_3); 1.34 (s, 6H, Mes CH_3). ^{13}C NMR (C_6D_6): δ 166.24, 153.77, 142.06, 135.35, 133.80, 132.25, 129.69, 128.67, 124.93, 122.00, 116.30, 80.85, 20.51, 18.74, 18.04. ^{19}F NMR (C_6D_6): δ −122.58 (dd, J = 15.3 Hz, J = 12.2 Hz, 2F); −154.30 (t, J = 19.1 Hz, 1F); −162.6 (overlapping spt, J =12.2 Hz, 2F). Elemental analysis was not attempted on this molecule because of its instability.

Synthesis of (DAP)Re(Cl)(O)Al$(C_6F_5)_3$. A 100 mL Schlenk flask was charged with (DAP)Re(O)Cl (100 mg, 0.164 mmol) and Al$(C_6F_5)_3$·(toluene) (102 mg, 0.164 mmol, 1 equiv) and dissolved in 15 mL of toluene under an inert atmosphere. The resulting orange solution was stirred at room temperature for 1 h. The solvent volume was then reduced to ∼5 mL in vacuo, and excess hexanes (30 mL) was cannula-transferred in the flask, which precipitated an orange powder. The resulting mixture was stirred for another 30 min. Excess solvent was then cannula-filtered, leaving the yellow powder in the flask, which was further dried in vacuo for 3 h. Isolated yield; 135 mg (0.119 mmol, 72%). ^{1}H NMR (C_6D_6): δ 6.80 (t, J = 8.0 Hz, 1H, NC_2H_2CH); 6.71 (s, 2H, Mes *meta*-H); 6.62 (s, 2H, Mes *meta*-H); 6.60 (d, J = 8.0 Hz, 2H, NC_2H_2CH); 5.43 (d, J = 21.0 Hz, 2H, Mes NCH_2); 4.83 (d, J = 21.0 Hz, 2H, Mes NCH_2); 2.19 (s, 6H, Mes CH_3); 2.06 (s, 6H, Mes CH_3); 1.16 (s, 6H, Mes CH_3). ^{19}F NMR (C_6D_6): δ −122.8 (m, 2F), −153.5 (m, 1F), −162.3 (m, 2F). The complex was not characterized by ^{13}C NMR due to its very poor solubility in benzene or toluene. Elemental analysis was not attempted on this molecule because of its instability.

Synthesis of (DAP)Re(Me)(O)Al$(C_6F_5)_3$. A 100 mL Schlenk flask was charged with (DAP)Re(O)Me (100 mg, 0.170 mmol) and Al$(C_6F_5)_3$·(toluene) (105 mg, 0.170, 1 equiv) and dissolved in 15 mL of toluene under an inert atmosphere. The resulting purple solution was stirred at room temperature for 1 h. The solvent volume was then reduced to ∼5 mL in vacuo, and excess hexanes (30 mL) was cannula-transferred in the flask, which precipitated an orange powder. The resulting mixture was stirred for another 30 min. Excess solvent was then

was removed by cannula filtration, leaving the light purple powder in the flask, which was further dried in vacuo for 3 h. Isolated yield: 107 mg (0.096 mmol, 56%). ^{1}H NMR (C_6D_6): δ 6.84 (t, J = 8.0 Hz, 1H, NC_2H_2CH); 6.70 (s, 2H, Mes *meta*-H); 6.66 (s, 2H, Mes *meta*-H); 6.47 (d, J = 8.0 Hz, 2H, NC_2H_2CH); 5.42 (d, J = 21.0 Hz, 2H, Mes NCH_2); 4.78 (d, J = 21.0 Hz, 2H, Mes NCH_2); 3.81 (s, 3H, $Re-CH_3$); 2.18 (s, 6H, Mes CH_3); 2.07 (s, 6H, Mes−CH_3); 1.05 (s, 6H, Mes CH_3). ^{13}C NMR (C_6D_6): δ 166.45, 152.85, 141.71, 135.88, 134.67, 132.84, 130.01, 129.49, 129.18, 115.92, 81.06, 20.66, 18.12, 17.25. ^{19}F NMR (C_6D_6, δ): −123.2 (dd, J = 15.1 Hz, J = 12.1 Hz, 2F); −154.3 (t, J = 19.1 Hz, 1F); −162.6 (overlapping m, 2F). Elemental analysis was not attempted on this molecule because of its instability.

Synthesis of (DAP)Re(Et)(O)Al(C_6F_5)$_3$. A 100 mL Schlenk flask was charged with (DAP)Re(O)Et (101 mg, 0.165 mmol) and Al(C_6F_5)$_3$·(toluene) (104 mg, 0.170, 1 equiv) and dissolved in 15 mL of toluene under an inert atmosphere. The resulting purple solution was stirred at room temperature for 1 h. The solvent volume was then reduced to ~5 mL in vacuo, and excess hexanes (30 mL) was cannula-transferred in the flask, which precipitated an orange powder. The resulting mixture was stirred for another 30 min. Excess solvent was then was removed by cannula filtration, leaving the light purple powder in the flask, which was further dried in vacuo for 3 h. Isolated yield: 134 mg (0.117 mmol, 70%). ^{1}H NMR (C_6D_6): δ 6.99 (t, J = 8.0 Hz, 1H, NC_2H_2CH); 6.87 (s, 2H, Mes *meta*-H); 6.70 (d, J = 8.0 Hz, 2H, NC_2H_2CH); 5.47 (d, J = 21.0 Hz, 2H, Mes NCH_2); 4.89 (d, J = 21.0 Hz, 2H, Mes NCH_2); 2.48 (bs, 6H, Mes CH_3); 2.26 (s, 6H, Mes CH_3); 1.35 (bs, 6H, Mes CH_3); 1.21 (bs, 3H, $Re-CH_2CH_3$). The methylene group of the Re-Et fragment was not observed, presumably due to the rapid bond rotation. ^{13}C NMR (C_6D_6): δ 166.20, 152.05, 148.80, 141.11, 137.51, 135.89, 134.74, 131.03, 129.18, 128.93, 128.16, 127.90, 127.65, 127.41, 125.29, 115.53, 81.03, 21.02, 20.436, 17.85, 17.05. ^{19}F NMR (C_6D_6, δ): −122.9 (dd, J = 15.1 Hz, J = 12.1 Hz, 2F); −154.2 (t, J = 19.1 Hz, 1F); −162.4 (overlapping m, 2F). Elemental analysis was not attempted on this molecule because of its instability.

Synthesis of (DAP)Re(H)(O)Al(C_6F_5)$_3$. A 50 mL Schlenk flask was charged with (DAP)Re(O)H (34 mg, 0.059 mmol) and Al(C_6F_5)$_3$·(toluene) (36.7 mg, 0.059 mmol, 1 equiv) and dissolved in 5 mL of toluene under an inert atmosphere. The resulting light brown solution was stirred at room temperature for 1 h. The solvent volume was then reduced to ~1 mL in vacuo, and excess hexanes (10 mL) was cannula-transferred in the flask, which precipitated an orange powder. The resulting mixture was stirred for another 30 min. Excess solvent was then removed by cannula filtration, leaving the light brown powder in the flask, which was further dried in vacuo for 3 h. Isolated yield: 22 mg (0.020 mmol, 34%). ^{1}H NMR (C_6D_6): δ 11.50 (bs, 1H, Re-H); 6.80 (t, J = 8.0 Hz, 1H, NC_2H_2CH); 6.70 (s, 2H, Mes *meta*-H); 6.66 (s, 2H, Mes *meta*-H); 6.42 (d, J = 8.0 Hz, 2H, NC_2H_2CH); 5.40 (d, J = 21.0 Hz, 2H, Mes NCH_2); 4.82 (d, J = 21.0 Hz, 2H, Mes NCH_2); 2.27 (s, 6H, Mes CH_3); 2.13 (s, 6H, Mes CH_3); 1.33 (s, 6H, Mes CH_3). ^{19}F NMR (C_6D_6): δ −123.2 (dd, J = 15.1 Hz, J = 12.1 Hz, 2F); −154.5 (t, J = 19.1 Hz, 1F); −162.7 (overlapping m, 2F). ^{13}C NMR (C_6D_6, δ): 167.8, 158.8, 135.8, 134.7, 129.5, 116.2, 85.6, 79.0, 20.5, 18.6, 17.9. Elemental analysis was not attempted on this molecule because of its instability.

■ ASSOCIATED CONTENT

Ⓢ Supporting Information

The Supporting Information is available free of charge on the ACS Publications website at DOI: 10.1021/acscatal.6b03313.

Additional NMR data and X-ray data for **2** and **5** (PDF)
Crystallographic data (CIF)
Crystallographic data (CIF)

■ AUTHOR INFORMATION

Corresponding Author

*E-mail for E.A.I.: eaison@ncsu.edu.

ORCID 🔾

Elon A. Ison: 0000-0002-2902-2671

Notes

The authors declare no competing financial interest.

■ REFERENCES

(1) (a) Stephan, D. W. *J. Am. Chem. Soc.* **2015**, *137*, 10018−10032. (b) Stephan, D. W.; Erker, G. *Angew. Chem., Int. Ed.* **2015**, *54*, 6400−6441. (c) Paradies, J. *Angew. Chem., Int. Ed.* **2014**, *53*, 3552−3557. (d) Houghton, A. Y.; Hurmalainen, J.; Mansikkamaki, A.; Piers, W. E.; Tuononen, H. M. *Nat. Chem.* **2014**, *6*, 983−988. (e) Stephan, D. W.; Erker, G. *Chem. Sci.* **2014**, *5*, 2625−2641. (f) Mahdi, T.; Stephan, D. W. *Angew. Chem., Int. Ed.* **2013**, *52*, 12418−12421. (g) Berke, H.; Jiang, Y. F.; Yang, X. H.; Jiang, C. F.; Chakraborty, S.; Landwehr, A. *Top. Curr. Chem.* **2013**, *334*, 27−57. (h) Lu, Z. P.; Ye, H. Y.; Wang, H. D. *Top. Curr. Chem.* **2012**, *334*, 59−80. (i) Stephan, D. W.; Erker, G. *Top. Curr. Chem.* **2013**, *332*, 85−110. (j) Chernichenko, K.; Madarasz, A.; Papai, I.; Nieger, M.; Leskela, M.; Repo, T. *Nat. Chem.* **2013**, *5*, 718−723. (k) Stephan, D. W. *Org. Biomol. Chem.* **2012**, *10*, 9747−9747. (l) Ghattas, G.; Chen, D. J.; Pan, F. F.; Klankermayer, J. *Dalton Trans.* **2012**, *41*, 9026−9028. (m) Stephan, D. W. *Org. Biomol. Chem.* **2012**, *10*, 5740−5746. (n) Soos, T. *Pure Appl. Chem.* **2011**, *83*, 667−675. (o) Berkefeld, A.; Piers, W. E.; Parvez, M. *J. Am. Chem. Soc.* **2010**, *132*, 10660−10661. (p) Eros, G.; Mehdi, H.; Papai, I.; Rokob, T. A.; Kiraly, P.; Tarkanyi, G.; Soos, T. *Angew. Chem., Int. Ed.* **2010**, *49*, 6559−6563. (q) Geier, S. J.; Stephan, D. W. *J. Am. Chem. Soc.* **2009**, *131*, 3476−3477. (r) Kim, H. W.; Rhee, Y. M. *Chem. - Eur. J.* **2009**, *15*, 13348−13355. (s) Chase, P. A.; Stephan, D. W. *Angew. Chem., Int. Ed.* **2008**, *47*, 7433−7437.

(2) (a) Lu, G.; Zhang, P.; Sun, D.; Wang, L.; Zhou, K.; Wang, Z.-X.; Guo, G.-C. *Chem. Sci.* **2014**, *5*, 1082−1090. (b) Greb, L.; Tussing, S.; Schirmer, B.; Ona-Burgos, P.; Kaupmees, K.; Lokov, M.; Leito, I.; Grimme, S.; Paradies, J. *Chem. Sci.* **2013**, *4*, 2788−2796. (c) Liu, Y.; Du, H. *J. Am. Chem. Soc.* **2013**, *135*, 6810−6813. (d) Lindqvist, M.; Sarnela, N.; Sumerin, V.; Chernichenko, K.; Leskela, M.; Repo, T. *Dalton Trans.* **2012**, *41*, 4310−4312. (e) Heiden, Z. M.; Stephan, D. W. *Chem. Commun.* **2011**, *47*, 5729−5731. (f) Axenov, K. V.; Momming, C. M.; Kehr, G.; Frohlich, R.; Erker, G. *Chem. - Eur. J.* **2010**, *16*, 14069−14073. (g) Rokob, T. A.; Hamza, A.; Stirling, A.; Papai, I. *J. Am. Chem. Soc.* **2009**, *131*, 2029−2036. (h) Chen, D.; Klankermayer, J. *Chem. Commun.* **2008**, 2130−2131.

(3) Wei, S.; Du, H. *J. Am. Chem. Soc.* **2014**, *136*, 12261−12264.

(4) (a) vom Stein, T.; Perez, M.; Dobrovetsky, R.; Winkelhaus, D.; Caputo, C. B.; Stephan, D. W. *Angew. Chem., Int. Ed.* **2015**, *54*, 10178−10182. (b) Whittemore, S. M.; Autrey, T. *Isr. J. Chem.* **2015**, *55*, 196−201. (c) Xu, X.; Kehr, G.; Daniliuc, C. G.; Erker, G. *J. Am. Chem. Soc.* **2015**, *137*, 4550−4557. (d) Dornan, P. K.; Longobardi, L. E.; Stephan, D. W. *Synlett* **2014**, *25*, 1521−1524. (e) Feldhaus, P.; Schirmer, B.; Wibbeling, B.; Daniliuc, C. G.; Frohlich, R.; Grimme, S.;

Kehr, G.; Erker, G. *Dalton Trans.* **2012**, *41*, 9135−9142. (f) Fromel, S.; Kehr, G.; Frohlich, R.; Daniliuc, C. G.; Erker, G. *Dalton Trans.* **2013**, *42*, 14531−14536. (g) Greb, L.; Daniliuc, C.-G.; Bergander, K.; Paradies, J. *Angew. Chem., Int. Ed.* **2013**, *52*, 5876−5879. (h) Menard, G.; Tran, L.; Stephan, D. W. *Dalton Trans.* **2013**, *42*, 13685−13691. (i) Nicasio, J. A.; Steinberg, S.; Ines, B.; Alcarazo, M. *Chem. - Eur. J.* **2013**, *19*, 11016−11020. (j) Paradies, J. *Synlett* **2013**, *24*, 777−780. (k) Wang, Y.; Chen, W.; Lu, Z.; Li, Z. H.; Wang, H. *Angew. Chem., Int. Ed.* **2013**, *52*, 7496−7499. (l) Xu, X.; Kehr, G.; Daniliuc, C. G.; Erker, G. *Organometallics* **2013**, *32*, 7306−7311. (m) Xu, X.; Kehr, G.; Daniliuc, C. G.; Erker, G. *Angew. Chem., Int. Ed.* **2013**, *52*, 13629−13632. (n) Yu, J. G.; Kehr, G.; Daniliuc, C. G.; Erker, G. *Eur. J. Inorg. Chem.* **2013**, *2013*, 3312−3315. (o) Greb, L.; Oña-Burgos, P.; Schirmer, B.; Grimme, S.; Stephan, D. W.; Paradies, J. *Angew. Chem.* **2012**, *124*, 10311−10315. (p) Zhao, X. X.; Stephan, D. W. *Chem. Sci.* **2012**, *3*, 2123−2132. (q) Zhao, X. X.; Stephan, D. W. *J. Am. Chem. Soc.* **2011**, *133*, 12448−12450. (r) Pàmies, O.; Andersson, P. G.; Diéguez, M. *Chem. - Eur. J.* **2010**, *16*, 14232−14240. (s) Momming, C. M.; Fromel, S.; Kehr, G.; Frohlich, R.; Grimme, S.; Erker, G. *J. Am. Chem. Soc.* **2009**, *131*, 12280−12289. (t) Sortais, J. B.; Voss, T.; Kehr, G.; Frohlich, R.; Erker, G. *Chem. Commun.* **2009**, 7417−7418. (u) Guo, Y.; Li, S. *Eur. J. Inorg. Chem.* **2008**, *2008*, 2501−2505. (v) Stirling, A.; Hamza, A.; Rokob, T. A.; Papai, I. *Chem. Commun.* **2008**, 3148−3150. (w) McCahill, J. S. J.; Welch, G. C.; Stephan, D. W. *Angew. Chem., Int. Ed.* **2007**, *46*, 4968−4971. (x) Herrmann, W. A.; Roesky, P. W.; Wang, M.; Scherer, W. *Organometallics* **1994**, *13*, 4531−4535.

(5) (a) Sajid, M.; Lawzer, A.; Dong, W.; Rosorius, C.; Sander, W.; Schirmer, B.; Grimme, S.; Daniliuc, C. G.; Kehr, G.; Erker, G. *J. Am. Chem. Soc.* **2013**, *135*, 18567−18574. (b) Miller, A. J. M.; Labinger, J. A.; Bercaw, J. E. *J. Am. Chem. Soc.* **2010**, *132* (10), 3301−3303.

(6) Kamlet, M. J.; Abboud, J. L. M.; Abraham, M. H.; Taft, R. *J. Org. Chem.* **1983**, *48*, 2877−2887.

(7) Lambic, N. S.; Sommer, R. D.; Ison, E. A. *J. Am. Chem. Soc.* **2016**, *138*, 4832−4842.

(8) (a) Lambic, N. S.; Lilly, C. P.; Robbins, L. K.; Sommer, R. D.; Ison, E. A. *Organometallics* **2016**, *35*, 2822−2829. (b) Britovsek, G. J.; Gibson, V. C.; Mastroianni, S.; Oakes, D. C.; Redshaw, C.; Solan, G. A.; White, A. J.; Williams, D. J. *Eur. J. Inorg. Chem.* **2001**, *2001*, 431−437.

(9) Parks, D. J.; Piers, W. E.; Yap, G. P. *Organometallics* **1998**, *17*, 5492−5503.

(10) Hair, G. S.; Cowley, A. H.; Jones, R. A.; McBurnett, B. G.; Voigt, A. *J. Am. Chem. Soc.* **1999**, *121*, 4922−4923.

(11) Lilly, C. P.; Boyle, P. D.; Ison, E. A. *Dalton Trans.* **2011**, *40*, 11815−11821.

(12) (a) Smeltz, J. L.; Lilly, C. P.; Boyle, P. D.; Ison, E. A. *J. Am. Chem. Soc.* **2013**, *135*, 9433−9441. (b) Lilly, C. P.; Boyle, P. D.; Ison, E. A. *Organometallics* **2012**, *31*, 4295−4301.

(13) Hounjet, L. J.; Bannwarth, C.; Garon, C. N.; Caputo, C. B.; Grimme, S.; Stephan, D. W. *Angew. Chem., Int. Ed.* **2013**, *52*, 7492−7495.

(14) See the Supporting Information for a space-filling model comparison of the two structures.

(15) As pointed out by a reviewer, the dynamic behavior may also be attributed to rotation of the $Al(C_6F_5)_3$ fragment about the Al−O bond. This possibility cannot be ruled out at this time.

(16) (a) Bradley, D. C.; Harding, I. S.; Keefe, A. D.; Motevalli, M.; Zheng, D. H. *J. Chem. Soc., Dalton Trans.* **1996**, 3931−3936. (b) Chakraborty, D.; Chen, E. Y. X. *Organometallics* **2003**, *22*, 207−210.

(17) Timoshkin, A. Y.; Frenking, G. *Organometallics* **2008**, *27*, 371−380.

(18) (a) Ménard, G.; Tran, L.; Stephan, D. W. *Dalton Trans.* **2013**, *42*, 13685−13691. (b) Ménard, G.; Stephan, D. W. *Angew. Chem., Int. Ed.* **2012**, *51*, 8272−8275.

(19) For recent examples of catalytic tuning of FLPs for CO_2 activation, see: (a) Fontaine, F.-G.; Courtemanche, M.-A.; Légaré, M.-A.; Rochette, É. *Coord. Chem. Rev.* **2016**, 10.1016/j.ccr.2016.05.005

(b) Declercq, R.; Bouhadir, G.; Bourissou, D.; Légaré, M.-A.; Courtemanche, M.-A.; Nahi, K. S.; Bouchard, N.; Fontaine, F.-G.; Maron, L. *ACS Catal.* **2015**, *5*, 2513−2520. (c) Courtemanche, M.-A.; Légaré, M.-A.; Maron, L.; Fontaine, F.-G. *J. Am. Chem. Soc.* **2014**, *136*, 10708−10717. (d) Courtemanche, M.-A.; Légaré, M.-A.; Maron, L.; Fontaine, F.-G. *J. Am. Chem. Soc.* **2013**, *135*, 9326−9329.